Evolutionary Computing Approach for Evaluating Flory Distribution Curves in Gel Permeation Chromatography: Study of the Poly(1-octene) System

Gurmeet Singh, Sukhdeep Kaur, Dhananjay G. Naik, Virendra K. Gupta

Catalyst and Material Reliance Technology Center, Reliance Industries, Limited, Hazira Complex, Surat 394510, Gujarat, India

Received 18 September 2009; accepted 2 January 2010
DOI 10.1002/app.32097
Published online 12 May 2010 in Wiley InterScience (www.interscience.wiley.com).

ABSTRACT: We carried out deconvolution of the molecular weight distribution curves from gel permeation chromatography for polyolefins into individual active sites considering Flory distribution by an evolutionary-computing-based real-coded genetic algorithm, a nonlinear multivariate optimization algorithm. We applied the deconvolution to homopolymers of 1-octene synthesized using heterogeneous Ziegler–Natta catalysts with different amounts of hydrogen. The molecular weight distribution was deconvoluted in to five Flory distributions, which showed a sensitivity to hydrogen amounts. With no hydrogen presence, the peaks corresponding to high-molecular-weight fractions were intense. As the amount of hydrogen was increased, not only did the intensities of the high-molecular-weight peaks decrease, but also peaks corresponding to low-molecular-weight fractions were observed. The method allowed us to determine the active site distribution of the polymer molecular weight distribution obtained from gel permeation chromatography.
 J Appl Polym Sci 117: 3379–3385, 2010

Key words: gel permeation chromatography (GPC); modeling; polyolefins

INTRODUCTION

The molecular weight distribution (MWD) of polymers is important, as it determines many of the physicochemical properties of polymers.[1,2] The toughness, hardness, stiffness, strength, and viscoelasticity are among some of the properties that are dependent on MWD. If the molecular weight is low, the mechanical properties and transition temperatures of the polymer will generally be insufficient for commercial applications, and if the molecular weight is too high, it poses problems during processing. Thus, for commercial applications of polymers, there needs to be balance in the distribution of low- and high-molecular-weight fractions for the desired processability window and load-bearing capabilities.

Gel permeation chromatography (GPC) and physical separation with selective solvent extraction at various temperatures are the tools used for the separation of polymer components.[3] Because of the high level of automation, sophistication, reliability, and reproducibility of GPC instrumentation, a much higher resolution of data can be produced for mechanistic studies in comparison to basic solvent extraction techniques; this makes it the best tool for understanding the MWD of polymers. The separation of the GPC curve into individual Flory distribution curves provides detailed information regarding the active site distribution on the basis of fractions that have distinct molecular weight profiles; this leads to a lot of insight into the polymerization mechanism.[4–14] The deconvolution of the MWDs of polymer resins, which is used for the characterization of polymer resins with broad and/or bimodal MWDs, has been carried out by various methodologies, such as the Haarhoff-Van der Linde function,[4] commercial software (Scientist,[5] Peakfit,[6] Microsoft Excel Solver[7]), and the Levenberg–Marquardt and Golub–Pereyra methods.[8]

A genetic algorithm, based on Darwin's theory of natural evolution, is a numerical optimization algorithm that is highly suited for large-scale optimization problems.[15–18] The advent of artificial-intelligence-based evolutionary programming has enabled us to tackle problems that are difficult to solve with traditional optimization techniques, including problems that are not well defined or are difficult to model mathematically, discontinuous, highly nonlinear, or stochastic. Genetic algorithms have found applications in a wide range of fields, including robotics, protein folding, and engineering design problems. Chemists have also started to benefit from these, as indicated by the increasing number of

Correspondence to: V. K. Gupta (virendrakumar.gupta@ril.com).

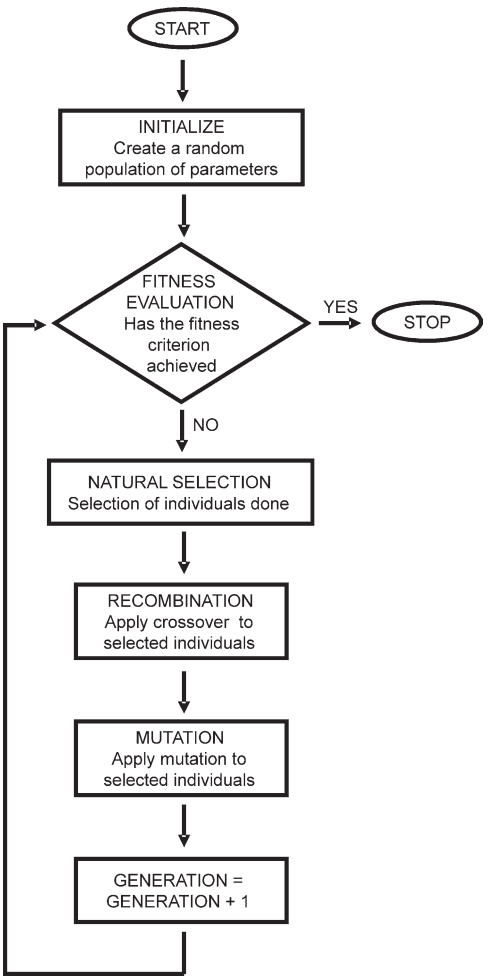

Figure 1 Flowchart of the genetic algorithm.

publications involving genetic algorithms, such as for automated wavelength selection,[19–22] reactivity ratio optimization,[23–26] and automated structure elucidation.[27–29] The algorithms provide several advantages over linear or traditional nonlinear optimization algorithms; for example, it works on generation principles whereby a number of data points are solved simultaneously, and the mutation subroutine provides a tool for moving from the local maxima or minima.[15–18]

The real-coded genetic algorithm (RCGA; Fig. 1) is initialized by the random generation of a set of parameters (population) to be optimized in the defined search space. In the next step, the parameters are selected on the basis of their fitness (how closely they resemble the solution). The selected parameters are further operated to generate the next generation of parameters with a crossover operation (the creation of the next generation). Some of the selected newly created parameters are subjected to mutation, whereby the parameters are extended in the search space to prevent stagnation/locking in the local domains. The algorithm scans the whole of the search space and evolves toward a global minima or maxima as required with each cycle of iteration. The algorithm continues until the parameters with the desired fitness are achieved or until a defined number of generations is crossed.

Heterogeneous Ziegler–Natta catalysts are complex systems for understanding, as there are number of components involved during polymerization. The basic factor over which everything revolves is the formation of active centers that are responsible for polymerization and stereospecificity. On the basis of the assumptions that, throughout polymerization, the reaction conditions remain constant and that the catalyst is a mixture of a finite number of different types of active sites, the MWD of the final polymer obtained may be described as the sum of a finite number of Flory distributions.[9]

It is well known that control over molecular weight is attainable through hydrogen during the Ziegler–Natta polymerization of α-olefins, as it behaves as a chain-transfer agent.[30–33] The intriguing fact here is that the catalyst sites responsible for the production of the lower molecular weight fractions are the ones affected by hydrogen more strongly. So, understanding the Flory distribution curves with changes in the hydrogen concentration can be challenging and provides deeper insight into the understanding of the active sites. In this article, we report the advantages and application of RCGA-based evolutionary computing for the deconvolution of GPC curves of poly(1-octene) to understand the effect of hydrogen concentration on the active sites.[34]

EXPERIMENTAL

Materials

1-Octene (98%, Aldrich, USA) was used as received. *n*-Decane (98%, Labort, India) and *n*-hexane (99%, Labort, India) were dried under nitrogen over molecular sieves. A triethylaluminum (Witco, Germany) solution was used at 10% (v/v) in *n*-decane. A $MgCl_2$-supported titanium catalyst (3.0 wt % Ti and 12 wt % diisobutyl phthalate) was used as a 3 wt % catalyst slurry.[35]

Polymerization

All work relating to the handling of air- and moisture-sensitive compounds were carried out in a nitrogen atmosphere with standard Schlenk techniques. A 1-L double-jacketed glass reactor equipped with a mechanical stirrer with a glass stirrer with a polytetrafluoroethylene blade was used to polymerize 1-octene. The polymerization assembly was kept

under nitrogen. Calculated amounts of *n*-hexane, triethylaluminum (cocatalyst), and 1-octene were added to the reactor. After the addition of the catalyst, the same amount of catalyst was taken in a volumetric flask for titanium estimation, which was used to calculate the amount of catalyst used for each polymerization. The reaction temperature was then set to the required degree. The polymerization was done for 2 h, after which the reaction was terminated by the addition of methanol containing 5 wt % HCl. The polymer was dried *in vacuo* at 60°C until a constant weight was reached. Polymerizations were performed at three different hydrogen concentrations [0 (PO-1), 0.02 (PO-2), and 0.14 mol (PO-3)] to determine the effect on the active site distributions. The reactor temperature was set to 70°C with the pressure at 5 kg/cm^2. After 2 h, the reaction was terminated by the addition of acidified methanol. The polymer was dried *in vacuo* at 60°C until a constant weight was reached.

GPC

The MWD of the polymers was determined by size exclusion chromatography with a Polymer Laboratories PL-GPC 220 high-temperature chromatograph instrument (columns: 3 × PLgel Mixed-B 10 μm) and two detectors (a viscometer and refractometer) in trichlorobenzene at flow rate of 1 mL/min at 145°C. The system was calibrated with polystyrene standards with universal calibration.

GPC deconvolution

Deconvolution of the GPC profile was done into Flory distribution curves with a genetic algorithm to optimize the Flory components. The code for the RCGA was written in C++ language. The iteration was carried for 500 generations to obtain optimized parameters with a population of 50 individuals.

RESULTS AND DISCUSSION

Flory distribution

The Flory distribution functions were applied to the polymerization processes with the following considerations:

1. The kinetic parameters were the same for all chain-propagating species.
2. The chain termination reaction probability did not depend on the chain length and was low.
3. The chain-propagating species concentration remained constant.
4. Polymerization reactions were carried out at constant concentrations of monomers and other chemical species that may have affected the molecular weight.[9]

The Flory theory states that the instantaneous number distribution function (F^*) of growing polymer chains with n monomer units is defined as follows:

$$F^*(n) = a\exp(-an) \tag{1}$$

where a is the ratio of the chain termination rate to the chain propagation rate and is constant for a polymerization and independent of n. It is defined as follows:

$$a = \sum R_t/R_p \tag{2}$$

where $\sum R_t$ is the summation of the chain termination rates and R_p is the chain propagation rate.

For most olefin polymerizations with $MgCl_2$-supported Ti-based Ziegler–Natta catalysts, with a constant monomer concentration and a single active center producing a large number of polymer chains, the degree of polymerization is $1/a$. The weight distribution function [$F(w)$], consisting of n monomer units, is defined as follows:

$$F(w) = \frac{nF(n)}{\int [nF(n)]} = a^2 n\exp(-an) \tag{3}$$

For the calculation of the theoretical GPC curve, as described by Kissin [9], eq. (3) and the assumption that a linear correlation exists between the retention times and the peaks of monodisperse polymer fractions leads to the following Flory distribution function in the GPC coordinates:

$$a^2n^2\exp(-an)\text{versus}\log\ n \tag{4}$$

The distribution function for an active site with fraction f becomes the following:

$$fa^2n^2\exp(-an)\text{versus}\log\ n \tag{5}$$

The factor f needs to be incorporated, as the intensity of each of the Flory distribution curve differs on the basis of the MWD of the polymer.

RCGA

To initialize the RCGA, a population of 50 uniformly distributed individuals or strings representing parameters to be optimized was randomly generated in the bounds of the predefined search space. The search space was defined for factor a as $0 < a < 0.04$ (on the basis of the MWD of the polymer samples

under consideration) and for factor f as $0 \leq f \leq 1$ to deconvolute the GPC curve with the Flory distribution as given by eq. (5). Each string was characterized by the values of a and f. The search space was, thus, $2 \times i$ dimensions for an i number of Flory distribution curves with a factor of 2 for a and f parameters for each Flory distribution curve.

In the next step, the strings were evaluated by the calculation of the value of the integral least-square difference between the theoretical and experimental curves (D):

$$D = \sum_{1}^{i} \{[fa^2n^2 \exp(-an)]_{\text{Theoretical}} - [fa^2n^2 \exp(-an)]_{\text{Experimental}}\}^2 \quad (6)$$

at different n values for i active sites for a given set of a and f for theoretical curves. The value of $[fa^2n^2\exp(-an)]_{\text{Experimental}}$ was obtained from the GPC data. The target was to minimize D and obtain the best fit between the theoretical and experimental GPC curves by the optimization of the a and f parameters for each active site. The strings were further operated by three operators, selection, crossover, and mutation, to create a new set of population (Fig. 1). The strings were selected for crossover on the basis of the fitness with a tournament selection operator. Randomly, b number of strings were selected, and c ($b > c$) number of better fitting strings (with lower D values) were carried over for crossover; with the number of selected strings maintained at 50. The selected strings were then allowed to produce the next generation, that is, to perform crossover to diversify the genetic makeup and to prevent stagnancy.

A heuristic crossover operator was applied on the selected strings for the crossover to generate next generation of population. The heuristic crossover operator uses the fitness values of the two parent strings to determine the direction of the search. The offspring strings are created according to the following equations (for values of a and f for each string):

$$X' = X + r(X - Y)$$
$$Y' = X \quad (7)$$

where X' and Y' are the progeny (next-generation strings), X and Y are parents with X being the better fitting parent, and r is a random number between 0 and 1.

To prevent the accidental trapping of individuals in the local minima, a nonuniform mutation operator was applied for mutation. This kept the population from stagnating in the early stages of the evolution and directed the probability of the mutation toward zero as the generation number increased and allowed

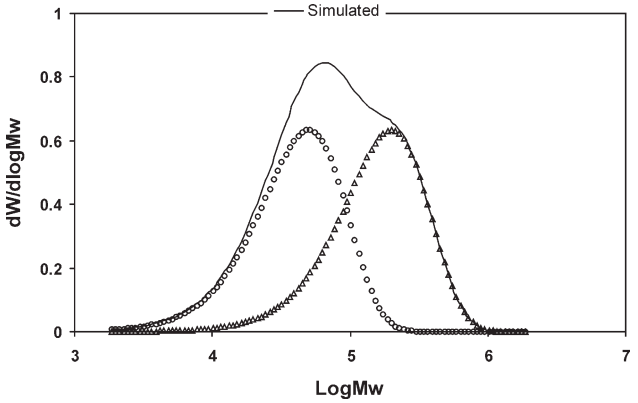

Figure 2 GPC MWD model of a polymer with two active sites.

the genetic algorithm to fine-tune the solution in the later stages of evolution. The nonuniform mutation is defined as follows:

$$X' = X + r_2(X_H - X)\left(1 - \frac{\text{Gen}}{\text{Gen}_{\max}}\right)^a \quad \text{if } r_1 < 0.5$$
$$X' = X - r_2(X - X_L)\left(1 - \frac{\text{Gen}}{\text{Gen}_{\max}}\right)^a \quad \text{if } r_1 \geq 0.5 \quad (8)$$

where X' and X are the individuals after and before the mutation, respectively; r_1 and r_2 are random numbers between 0 and 1; X_L and X_H are the lower and upper bounds for the X parameter (e.g., for factor f, $0 \leq f \leq 1$), respectively; Gen is the number of current generations; and $\text{Gen}_{\max}$ is the maximum number of generations.

Individuals move toward increasingly optimal solutions over generations and make the genetic algorithm highly probable for finding optimal solutions to a mathematical problem for which there may not be one correct answer. The functioning of the genetic algorithm is demonstrated by a hypothetical case of a bimodal polymer (Fig. 2) with two equally productive active sites ($f_1 = f_2 = 0.5$ and $a_1 = 0.00448$ and $a_2 = 0.001122$). For the purpose of clarity, only the optimization of f is illustrated in Figure 3 for the two-site model in a two-dimensional search space. In the first generation, the strings (f_1 and f_2) were generated in the defined search space. Within 10 generations, the strings were observed to be converging, although in local minima. At this stage, the mutation played the critical role, and by the 20th generation, some of the strings migrated to new dimensions and moved toward the global minima. The migration was evident in the 100th generation, and by the 250th generation, the evolution moved most of the population toward the global minima. The mutation operator now limited the divergence of the population, and thus, by the 250th generation, most of the individuals converged at the global

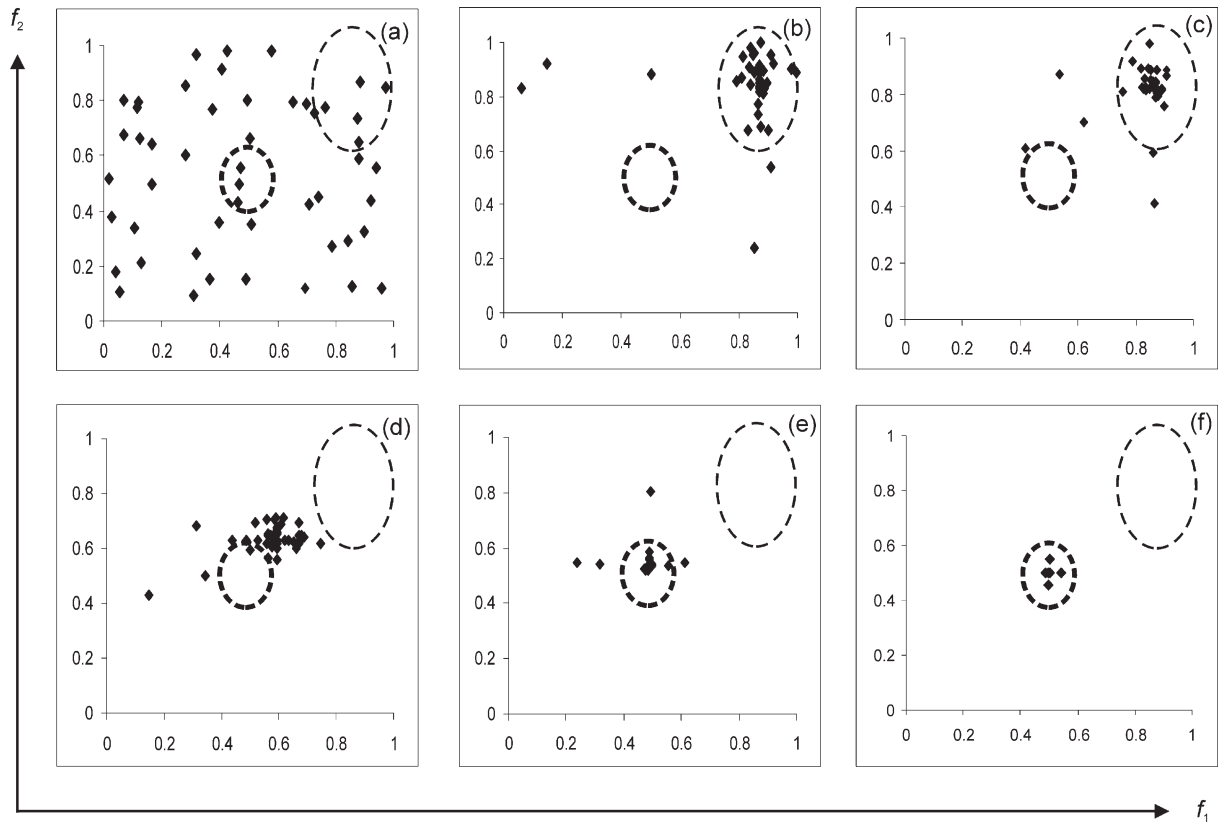

Figure 3 Critical effect of the mutation on the optimization of the parameters with the evolution of 50 individuals at (a) 1, (b) 10, (c) 25, (d) 50, (e) 100, and (f) 250 generations. The local minima are indicated by thick, dashed circles, and the global minima are indicated by thin, dashed circles.

minima. This characteristic feature and its capability to narrow down to good fitness after a small number of function evaluations prompted the application of the genetic algorithm for the optimization of the Flory parameters for GPC deconvolution.

GPC deconvolution of poly(1-octene)

The MWDs obtained by the molecular weight analysis of poly(1-octene) through GPC were deconvoluted into Flory distribution fractions with RCGA methodology. For the understanding of different active site variation and distribution relative to the hydrogen as a chain-transfer agent, the high-pressure slurry polymerization of 1-octene were conducted at an Al/Ti molar ratio of 250 with an $MgCl_2$-supported $TiCl_4$ catalyst having diisobutyl phthalate as an internal donor. The high-pressure polymerizations were done at PO-1, PO-2, and PO-3, respectively.

The MWD curves for poly(1-octene) samples were deconvoluted into five Flory components, and that five-site deconvolution provided a good fit of the tails of the MWDs. Here, one assumption, that each Flory component corresponded to a polymer produced on a certain type of active center, was made on the basis of the consideration that the polymerizations were conducted under mild conditions in solution and that the influences of diffusion limitation on MWD were neglected. This was helpful in terms of figuring out the distribution of active sites and the location of the position and relative peak intensity of each deconvoluted Flory component.

The optimized a and f parameters of the individual Flory components are given in Table I, along with the value of the weight-average molecular weight (M_w), which corresponded to the maximum of the given Flory component. The Flory curves (peaks) were located in a specific range of molecular weights to attain comparative information. For example, peaks I were located in the molecular weight range 9×10^5 to 10×10^5 corresponding to highest molecular weight range, peaks II were in the range 27×10^4 to 32×10^4, peaks III were in the range 11×10^4 to 12×10^4, peaks IV were in the range 37×10^3 to 43×10^3, and peaks V were in the range 10×10^3 to 12×10^3 corresponding to low molecular weights.

An examination of the data showed that, for the polymer synthesized in the absence of hydrogen as chain-transfer agent [Fig. 4(a)], peaks I–IV were observed, where peaks I and II correspond to active

TABLE I
Resolution of the GPC Curves into Individual Flory Components

	PO-1			PO-2			PO-3		
Active site	*a*	*f*	M_w	*a*	*f*	M_w	*a*	*f*	M_w
I	0.00025	0.43	908900	0.00022	0.01	1,035,800	—	0.00	—
II	0.00069	0.30	324100	0.00073	0.32	308,400	0.00084	0.14	267,500
III	0.00190	0.20	118000	0.00201	0.46	111,700	0.00190	0.43	118,100
IV	0.00564	0.07	39800	0.00603	0.18	37,200	0.00522	0.37	43,000
V	0.02152	0.00	10400	0.02140	0.03	10,500	0.01850	0.06	12,100

sites producing high-molecular-weight fractions. With the introduction of hydrogen (0.02 mol), peak V, which corresponded to the lowest molecular weight fraction having a low intensity, appeared as shown in Figure 4(b). As the amount of hydrogen was further increased (0.14 mol), peak I disappeared completely, and peaks II–V were observed [Fig. 4(c)].

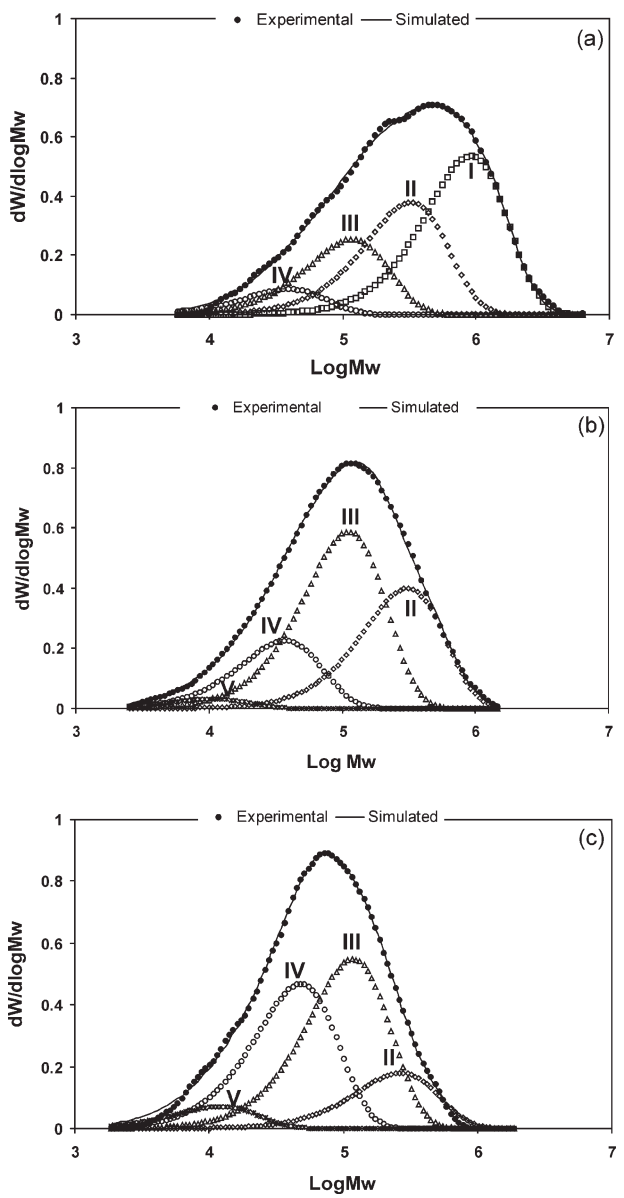

Figure 4 Deconvoluted Flory distribution curves for GPC of poly(1-octene) synthesized at (a) PO-1, (b) PO-2, and (c) PO-3.

To further understand the influence of the hydrogen amount, the value of parameter *f*, corresponding to the intensities (fraction) of these five Flory peaks for the three experiments conducted and given in Table I, was studied. At PO-1, where hydrogen was absent, peak I, which corresponded to the highest molecular weight fractions, had its maximum intensity. Also, the intensities of the peaks decreased from peak I to IV; this means that, when hydrogen was not present, the active sites responsible for producing high molecular weight were more prominent. With the introduction of hydrogen (PO-2), the intensity of peak I decreased drastically, and those of peaks III and IV increased. Also, peak V, corresponding to the lowest molecular fractions, although having a low intensity, appeared. This clearly indicated that, when hydrogen was used as chain-transfer agent, the active sites responsible for low molecular weight were affected. To further substantiate these assumptions, with a further increase in the hydrogen amount (PO-3), the intensities of peaks IV and V increased, although peak I disappeared completely; this indicated that the assumptions made were correct.

CONCLUSIONS

Deconvolution of the GPC profile into Flory distribution was performed by the fitting of the chromatogram into separate curves corresponding to the different molecular weight polymer fractions. RCGA-based nonlinear, multivariate least-squares methodology was used to fit the experimental data points to the theoretically calculated data points to optimize the Flory parameters for the individual curves. The strength of the RCGA was highlighted on the basis of its capability to evolve from the local minima and search the global minimum. The results indicate the applicability of the methodology for the deconvolution of the GPC profile into Flory distributions for the analysis of the active site distribution and correlation with mechanistic aspects of 1-octene polymerization. A strong correlation of the active center

distribution with hydrogen concentration as a chain-transfer agent was demonstrated.

References

1. Latado, A.; Embiruçu, M.; Neto, A. G. M.; Pinto, J. C. Polym Test 2001, 20, 419.
2. Nele, M.; Pinto, J. C. Macromol Theor Simul 2002, 11, 293.
3. Kissin, Y. V.; Chadwick, J. C.; Mingozzi, I.; Morini, G. Macromol Chem Phys 2006, 207, 1344.
4. D'Agnillo, L.; Soares, J. B. P.; Penlidis, A. J Polym Sci Part A: Polym Chem 1998, 36, 831.
5. Kissin, Y. V.; Ohnishi, R.; Konkazawa, T. Macromol Chem Phys 2004, 205, 284.
6. Vickroy, V. V.; Schneider, H.; Abbott, R. F. J Appl Polym Sci 1993, 50, 551.
7. Alghyamah, A. A.; Soares, J. B. P. Macromol Rapid Commun 2009, 30, 384.
8. Soares, J. B. P.; Hamielec, A. E. Polymer 1995, 36, 2257.
9. Kissin, Y. V. J Polym Sci Part A: Polym Chem 1995, 33, 227.
10. Fortuny, M.; Nele, M.; Melo, P. A.; Pinto, J. C. Macromol Theor Simul 2004, 13, 355.
11. Thompson, D. E.; McAuley, K. B.; McLellan, P. J. Macromol React Eng 2007, 1, 523.
12. Thompson, D. E.; McAuley, K. B.; McLellan, P. J. Macromol React Eng 2007, 1, 264.
13. Kissin, Y. V. J Polym Sci Part A: Polym Chem 2003, 41, 1745.
14. Maschio, G.; Scali, C. Makromol Chem Phys 1999, 200, 1708.
15. Holland, J. Adoption in Natural and Artificial Systems; University of Michigan Press: Ann Arbor, MI, 1975.
16. Goldberg, D. E. Genetic Algorithms in Search, Optimization, and Machine Learning; Addison-Wesley: Reading, MA, 1989.
17. Banzhaf, W.; Nordin, P.; Keller, R. E.; Francone, F. D. Genetic Programming: An Introduction: On the Automatic Evolution of Computer Programs and Its Applications; Morgan Kaufmann: San Francisco, 1997.
18. Deb, K. Optimization for Engineering Design: Algorithms and Examples; Prentice Hall: New Delhi, 2002.
19. Shaffer, R. E.; Small, G. W.; Arnold, M. A. Anal Chem 1996, 68, 2663.
20. Bangalore, A. S.; Shaffer, R. E.; Small, G. W.; Arnold, M. A. Anal Chem 1996, 68, 4200.
21. Ding, Q.; Small, G. W. Anal Chem 1998, 70, 4472.
22. Dane, A. D.; Timmermans, P. A. M.; van Sprang, H. A.; Buydens, L. M. C. Anal Chem 1996, 68, 2419.
23. Monett, D.; Méndez, J. A.; Abraham, G. A.; Gallardo, A.; Román, J. S. Macromol Theory Simul 2002, 11, 525.
24. Brar, A. S.; Singh, G.; Shankar, R. Eur Polym J 2004, 40, 2679.
25. Brar, A. S.; Singh, G.; Shankar, R. Polymer 2005, 46, 7164.
26. Brar, A. S.; Singh, G.; Shankar, R. Eur Polym J 2005, 41, 747.
27. Meiler, J.; Will, M. J Am Chem Soc 2002, 124, 1868.
28. Cooper, L. R.; Corne, D. W.; Crabbe, M. J. C. Comp Biol Chem 2003, 27, 575.
29. Hartnett, M.; Diamond, D. Anal Chem 1997, 69, 1909.
30. Chien, J. C. W.; Nozaki, T. J Polym Sci Part A: Polym Chem 1991, 29, 505.
31. Kissin, Y. V.; Rishina, L. A. J Polym Sci Part A: Polym Chem 2002, 40, 1353.
32. Kissin, Y. V.; Rishina, L. A.; Vizen, E. I. J Polym Sci Part A: Polym Chem 2002, 40, 1899.
33. Shimizu, F.; Pater, J. T. M.; Weickert, G. J Appl Polym Sci 2001, 81, 1035.
34. Kaur, S.; Naik, D. G.; Singh, G.; Patil, H. R.; Kothari, A. V.; Gupta, V. K. J Appl Polym Sci 2010, 115, 229.
35. Singh, G.; Kaur, S.; Makwana, U.; Patankar, R. B.; Gupta, V. K. Macromol Chem Phys 2009, 210, 69.